Mon. Not. R. Astron. Soc. **363,** 112–120 (2005) doi:10.1111/j.1365-2966.2005.09412.x

Correlation between radio luminosity and X-ray timing frequencies in neutron star and black hole X-ray binaries

S. Migliari,[1⋆] R. P. Fender[1,2] and M. van der Klis[1]

[1]*Astronomical Institute 'Anton Pannekoek', University of Amsterdam, and Center for High-energy Astrophysics, Kruislaan 403, 1098 SJ, Amsterdam, the Netherlands*

[2]*School of Physics and Astronomy, University of Southampton, Southampton, Hampshire SO17 1BJ*

Accepted 2005 July 11. Received 2005 July 11; in original form 2005 May 27

ABSTRACT

We report on correlations between radio luminosity and X-ray timing features in X-ray binary systems containing low magnetic field neutron stars and black holes. The sample of neutron star systems consists of 4U 1728–34, 4U 1820–34, Ser X-1, MXB 1730-335, GX 13+1, the millisecond X-ray pulsars SAX J1808.4-3658 and IGR J00291+5934, and these are compared with the black hole system GX 339–4. The analysis has been performed using data from pointed observations of the *Rossi X-ray Timing Explorer* coordinated with radio observations. In the neutron star systems the radio luminosity $L_{\rm R}$ is correlated with the characteristic frequency of the L_h Lorentzian component detected contemporaneously in the power spectrum, and anticorrelated with its strength. Similarly, in the black hole system GX 339–4 $L_{\rm R}$ is correlated with the frequency of the L_ℓ component in the power spectrum and anticorrelated with its strength. The index of a power-law fit to the correlation is similar in both cases, $L_{\rm R} \propto \nu^{\sim 1.4}$ and $L_{\rm R} \propto ({\rm rms})^{-2.3}$. At lower timing frequencies, the radio luminosity is further found to be correlated with the characteristic (break) frequency of the $L_{\rm b}$ component of the power spectra in the neutron stars and, marginally, with the equivalent break frequency in GX 339–4. We briefly discuss the coupling between the innermost regions of the accretion disc and the production of the jet and, from the behaviour of the millisecond accreting X-ray pulsars, the possible role of the neutron star magnetic field.

Key words: accretion, accretion discs – black hole physics – stars: neutron – ISM: jets and outflows – X-rays: binaries.

1 INTRODUCTION

Jet production in X-ray binaries (XRBs) is strongly related to the properties of the accretion disc. Recent works have established a link between the disc X-ray power and the jet radio power in black hole (BH) and neutron star (NS) XRB systems. In BH XRBs a non-linear correlation links the radio and the X-ray luminosity when in the hard state (e.g. Corbel et al. 2003; Gallo, Fender & Pooley 2003). Accretion disc and jet theories can translate this coupling into a relation between the power in the jet and mass accretion rate ($\dot{M}$). Heinz & Sunyaev (2003) have derived a non-linear relation between the radio power of the jet observed at a given frequency, the mass of the compact object and the mass accretion rate. In the case of BHs, it is common practice to convert the (bolometric) X-ray luminosities into Eddington units, and infer the mass accretion rate, that is the luminosity is a direct estimator of $\dot{M}$, although, as predicted already by, for example, the ADAF model (e.g. Narayan & Yi 1994, 1995; Narayan, Garcia & McClintock 1997), observationally the relation between luminosity and other $\dot{M}$ indicators is not straightforward (Homan et al. 2001; see also Homan & Belloni 2005; McClintock & Remillard 2005; Remillard 2005). In the case of NSs, the relation between the X-ray luminosity and other mass accretion rate indicators is definitely not one-to-one. Parallel tracks are observed in NS XRBs, both for individual sources and across sources, between the centroid frequency of the kHz quasi-periodic oscillations (QPOs) in the X-ray power spectra and the X-ray luminosity (e.g. Méndez et al. 1999; Ford et al. 2000; van der Klis 2001). QPOs are thought to be related to accretion disc properties (e.g. Miller & Homan 2004), and in particular kHz QPO frequencies are generally interpreted as being related to the motion of matter in the accretion disc at a preferential radius (see, e.g., van der Klis 2005 for a review). This suggests that the kHz QPOs may be a more direct indicator, rather than luminosity, at least of accretion geometry (see van der Klis 2001). Many works showed that the characteristic frequencies of the kHz QPOs are strongly related to the characteristic frequencies of the other timing features in the power spectra, so that lower-frequency QPOs (which are much easier to detect than the kHz ones) can be used as a proxy (e.g. Psaltis, Belloni & van der Klis 1999; Belloni,

⋆E-mail: migliari@science.uva.nl

Psaltis & van der Klis 2002; van Straaten et al. 2002; van Straaten, van der Klis & Méndez 2003; van Straaten, van der Klis & Wijnands 2005).

A positive correlation between radio and X-ray flux, reminiscent of that found in BH XRBs, has been found in the atoll-type NS 4U 1728–34 when in its hard X-ray state (Migliari et al. 2003; see Hasinger & van der Klis 1989 for a classification of NSs). Eight atolls and low-luminosity NS XRBs (compared with Z-type NSs) have been detected in the radio band so far, during coordinated radio and X-ray observations: 4U 1728–34 when steadily in its hard state (Migliari et al. 2003), 4U 1820–34 and Ser X-1 when steadily in their soft states (Migliari et al. 2004), Aql X-1 during an X-ray outburst (Rupen, Mioduszewski & Dhawan 2004), MXB 1730–335 (the Rapid Burster) during X-ray outbursts (Rutledge et al. 1998; Moore et al. 2000), the two millisecond accreting X-ray pulsars SAX J1808.4–3658 and IGR J00291+5934 during X-ray outbursts (Gaensler, Stappers & Getts 1999; Rupen et al. 2002; Pooley 2004). The 'peculiar' atoll source GX 13+1, is difficult to classify through X-ray analysis, having some X-ray properties of Z-type and some of atoll-type sources (but more likely to be identified as a bright atoll source: Schnerr et al. 2003), has also been detected at radio wavelengths, and shows a radio luminosity similar to (i.e. as strong as) that of Z sources (Homan et al. 2004).

2 OBSERVATIONS AND DATA ANALYSIS

We have inspected all the available X-ray observations with the Proportional Counter Array (PCA) on-board the *Rossi X-ray Timing Explorer* (*RXTE*), coordinated with radio observations (see Table 1) of atoll-type and millisecond accreting X-ray pulsars with a detected radio counterpart, i.e. 4U 1728–34, 4U 1820–34, Ser X-1, MXB 1730–335, GX 13+1, SAX J1808.4–3658 and IGR J00291+5934, and of the BH GX 339–4 in the hard state from Corbel et al. (2000). Throughout the paper we will use a 'broader' definition of atoll sources as (non-pulsating) low-magnetic field NS XRBs accreting at low-mass accretion rates (compared with Z-type NSs), which in this specific case also includes MXB 1730–335 (the Rapid Burster). Therefore, hereafter we will divide the sample into atolls and millisecond accreting X-ray pulsars. This is a more simplified definition (see van der Klis 2005 for a more detailed classification), but it is appropriate for the discussion in this paper. All of the observations in our sample, with dates, radio flux densities at 8.5 GHz and the best-fitting values of the characteristic frequencies of X-ray low-frequency features are shown in Table 2.

Table 1. Name of the source, date of the beginning of the observation and Obs. ID of the PCA/*RXTE* observation.

Source	Date	Obs. ID
	Neutron stars	
4U 1728–34	2000 May 05	50023-01-14-00
	2000 May 13	50023-01-16-00
	2000 May 21	50023-01-19-00
	2001 May 29	60029-02-02-00
	2001 Jun 01	60029-02-03-00
	2001 Jun 03	60029-02-04-00
	2001 Jun 05	60029-02-05-00
	2001 Jun 07	60029-02-06-00
	2001 Jun 09	60029-02-07-00
4U 1820–30	2002 Jul 25	70030-03-01-01
Ser X-1	2002 May 27	70027-04-01-00
MXB 1730–335	1996 Nov 6	20093-01-01-00
SAX J1808.4–3658	1998 Apr 27	30411-01-10-01
	2002 Oct 16	70080-01-01-04
	2002 Oct 18	70080-01-02-01
IGR J00291+5934	2004 Dec 6	90425-01-01-02
GX 13+1	1999 Aug 1	40022-01-01-01
	1999 Aug 4	40022-01-02-000
	Black hole	
GX 339–4	1997 Feb 4	20181-01-01-00
	1997 Feb 11	20181-01-02-00
	1997 Feb 18	20181-01-03-00
	1999 Mar 3	40108-01-04-000
	1999 Apr 2	40108-02-01-00
	1999 Apr 22	40108-02-02-00
	1999 May 14	40108-02-03-00

2.1 X-ray timing analysis

For NSs, we have used *event* data with a time resolution of 125 μs (E_125us_64M_0_1s) for the production of the power spectra of 4U 1728–34, 4U 1820–30, Ser X-1 and IGR J00291+5934, and of 16 μs (E_16us_64M_0_1s) for MXB 1730–335 (the Rapid Burster) and SAX J1808.4–3658. We used time bins such that the Nyquist frequency is 4096 Hz. For each observation we created power spectra from segments of 16 s (of 256 s for IGR J00291+5934) length using fast Fourier transform techniques (van der Klis 1989 and references therein) and we removed data drop-outs and X-ray bursts from the data, but no background subtraction was performed. No deadtime corrections were performed before creating the power spectra. We averaged the Leahy-normalized power spectra (Leahy et al. 1983) and subtracted the predicted Poisson noise spectrum by applying the method of Zhang et al. (1995), shifted in power to match the spectrum between 3000 and 4000 Hz. We converted the normalization of the power spectra to squared fractional rms (e.g. van der Klis 1995).

For the BH GX 339–4, we have used the same procedures as for NS. We used combined *binned* (B_250us_2A_0_13_Q), *single-bit* (SB_250us_14_17_2s) and *event* (E_250us_128M_18_8s) data with a time resolution of 250 μs for the production of power spectra and a Nyquist frequency of 2048 Hz. We created power spectra from segments of 128 s, averaged them and subtracted the predicted Poisson noise spectrum shifted in power to match the spectrum between 1000 and 2048 Hz.

We have fitted all the power spectra with a multi-Lorentzian model (e.g. Belloni et al. 2002 and references therein), and plotted in the νP_ν representation (with P_ν the normalized power and ν the frequency). In this representation the Lorentzian component attains its maximum at the characteristic frequency $\nu_{\max}$. The frequencies quoted here are therefore all $\nu_{\max}$ values, where $\nu_{\max} = (\nu_0^2 + \Delta^2)^{1/2}$ (ν_0 is the centroid frequency of the Lorentzian and Δ is the half-width at half maximum), which are comparable to the central frequencies values ν_0 for sharp (quality factor $Q = \nu_0/\mathrm{FWHM} \geqslant 2$, where FWHM is the full width at half maximum) features (Belloni et al. 2002).

The features in the power spectra have been identified and labelled based on the works of Psaltis et al. (1999), Belloni et al. (2002), van Straaten et al. (2002, 2003, 2005), Altamirano et al. (2005), Linares et al. (2005), Klein-Wolt, van Straaten & van der Klis (in preparation; see Klein-Wolt 2004).

2.2 The sample

4U 1728–34. Migliari et al. (2003) reported a correlation between radio flux densities and the characteristic frequency of the X-ray

Table 2. Name of the source, date of the beginning of the radio observations coordinated with X-rays, flux density at 8.46 GHz, characteristic frequency of L_{b2}, L_b and L_h (L_{break}, L_h and L_ℓ for the black hole), the distance to the source and the references. Errors on the radio flux are 1σ, errors on frequencies and rms are 90 per cent statistical errors.

			Neutron stars				
Source	Obs. date	$F_{8.5}$ (mJy)	ν_{b2}	ν_b	ν_h	D (kpc)	Ref.
4U 1728–34	2000 May 05	0.6 ± 0.2	16.14 ± 3.82	22.35 ± 0.72	48.12 ± 2.07	4.6	M03,G03
	2000 May 13	0.33 ± 0.08	5.70 ± 0.66	15.77 ± 0.57	27.84 ± 1.45		
	2000 May 21	0.62 ± 0.10	7.16 ± 0.49	18.43 ± 0.47	30.14 ± 1.68		
	2001 May 29	0.11 ± 0.02	–	2.67 ± 0.23	15.64 ± 0.53		
	2001 Jun 01	0.09 ± 0.02	–	2.36 ± 0.58	13.13 ± 1.45		
	2001 Jun 03	0.11 ± 0.02	–	1.50 ± 0.23	13.89 ± 1.19		
	2001 Jun 05	0.15 ± 0.02	–	1.62 ± 0.18	10.95 ± 0.55		
	2001 Jun 07	0.16 ± 0.02	–	1.94 ± 0.28	11.78 ± 0.71		
	2001 Jun 09	0.09 ± 0.02	–	1.37 ± 0.11	8.37 ± 0.36		
4U 1820–30	2002 Jul 25	0.138 ± 0.035	9.15 ± 2.38	23.42 ± 0.75	–	7.6	M04,H00
Ser X-1	2002 May 27	0.076 ± 0.015	15.50 ± 1.83	30.56 ± 0.76	67.07 ± 2.11	12.7	M04,JN04
MXB 1730–335	1996 Nov 6	0.370 ± 0.045	8.08 ± 4.04	17.21 ± 1.13	60.08 ± 2.71	8.8	M00, K03
SAX J1808.4–3658	1998 Apr 27	0.8 ± 0.18	–	0.814 ± 0.100	–[a]	2.5	G99,Z01
	2002 Oct. 16	0.44 ± 0.06	4.50 ± 1.72	14.62 ± 0.44	76.30 ± 2.03		R02
	2002 Oct. 18	0.30 ± 0.08	–	4.53 ± 0.55	21.43 ± 0.40		
IGR J00291+5934	2004 Dec 6[b]	0.180 ± 0.035[c]	0.052 ± 0.006	0.69 ± 0.08	4.86 ± 0.94	4	G05,F04
GX 13+1	1999 Aug 1	0.25 ± 0.05	–	4.45 ± 0.66	–	7	GS86,H04
	1999 Aug 4	$0.9 - 5.2$[d]	–	11.86 ± 1.68	56.86 ± 2.63		
			Black hole				
Source	Obs. date	$F_{8.5}$ (mJy)	ν_{break}	ν_h	ν_ℓ	D (kpc)	Ref.
GX 339–4	1997 Feb 4	9.10 ± 0.10	0.102 ± 0.013	0.50 ± 0.02	3.89 ± 0.09	$t > 7$	C00,H04
	1997 Feb 11	8.20 ± 0.10	0.107 ± 0.014	0.43 ± 0.02	3.67 ± 0.07		Z04
	1997 Feb 18	8.70 ± 0.20	0.085 ± 0.010	0.42 ± 0.01	3.63 ± 0.06		
	1999 Mar 3	5.74 ± 0.06	0.095 ± 0.009	0.60 ± 0.01	4.32 ± 0.13		
	1999 Apr 2	5.10 ± 0.07	0.080 ± 0.015	0.35 ± 0.02	3.11 ± 0.14		
	1999 Apr 22	3.11 ± 0.04	0.037 ± 0.011	0.21 ± 0.06	2.57 ± 0.07		
	1999 May 14	1.44 ± 0.04	–	0.05 ± 0.01[e]	1.41 ± 0.12		

[a]The power spectrum of this observation allows one to identify L_b at ∼0.8 Hz, but due to the poor statistics above 4 Hz only a broad feature can be fitted at ∼17 Hz (see van der Klis 2004).
[b]The date refers to the start of the radio observation, the public *RXTE* observation we have analysed started on December 7, a few hours after the end of the radio observations.
[c]The flux density of 0.250 ± 0.035 mJy at 5 GHz (Fender et al. 2004) has been converted to a flux density at 8.5 GHz assuming an optically thin spectrum with spectral index $\alpha = -0.6$ ($S_\nu \propto \nu^\alpha$, where S_ν is the radio flux density observed at a frequency ν).
[d]The radio emission during the flare has been converted to 8.5 GHz assuming an optically thin radio spectrum with $\alpha = -0.6$ (e.g. Hjellming et al. 1990a,b; Cooke & Ponman 1991; Penninx et al. 1993; Fomalont et al. 2001).
[e]The identification is ambiguous between L_h (more likely) and L_{break}.
References. M03, Migliari et al. (2003); G03, Galloway et al. (2003); H00, Heasley et al. (2000); M04, Migliari et al. (2004); JN04, Jonker & Nelemans (2004); M00, Moore et al. (2000); K03, Kuulkers et al. (2003) and references therein; G99, Gaensler et al. (1999); Z01, in't Zand et al. (2001); R02, Rupen et al. (2002); G05, Galloway et al. (2005); F04, Fender et al. (2004); C01, Corbel et al. (2000); H04, Hynes et al. (2004); Z04, Zdziarski et al. (2004).

low-frequency QPOs. We used the values of the radio flux density at 8.5 GHz (taken with the Very Large Array, VLA) listed in their table 1. The power spectra were fitted using one broad Lorentzian to represent the low-frequency noise and the break frequency (L_b or L_{b2}), one or two narrower Lorentzians (L_b and L_h) below ∼50 Hz, a broad Lorentzian around 100 Hz ($L_{h\ \mathrm{Hz}}$) and narrow Lorentzians to fit the kHz QPOs. A typical power spectrum of 4U 1728–34 is shown in Fig. 1. The identification of the features has been made using van Straaten et al. (2002).

4U 1820–30. Migliari et al. (2004) reported a radio detection (with the VLA) at 8.5 GHz of the source when steadily in its soft (lower banana, LB) X-ray state. Only on 2002 July 25, among the seven simultaneous radio/X-ray observations of 4U 1820–30 taken every 2–3 d, the radio source was significantly detected (∼4σ, although an average over the seven days of radio observations gives a 5σ level detection). The power spectrum of the PCA/*RXTE* observation on this date is shown in Fig. 1. We needed three Lorentzians to fit the power spectrum: a broad Lorentzian to fit the very low-frequency noise (VLFN), L_{b2} at approximately 9 Hz and L_b around 23 Hz. The identification of the features has been made using van Straaten et al. (2002, 2003, 2005) and Altamirano et al. (2005).

Ser X-1. Migliari et al. (2004) reported the discovery (with the VLA) of the radio counterpart of Ser X-1 at 8.5 GHz, while the source was steadily in its soft (LB) X-ray state. The power spectrum of the PCA/*RXTE* observation simultaneous with the radio band is shown in Fig. 1. We have fitted the power spectrum of Ser X-1 with four Lorentzians: a broad Lorentzian for the VLFN, L_{b2} at ∼15 Hz, L_b ∼ 30 Hz and L_h at ∼70 Hz. The identification of the features has been made using van Straaten et al. (2002, 2003, 2005) and Altamirano et al. (2005).

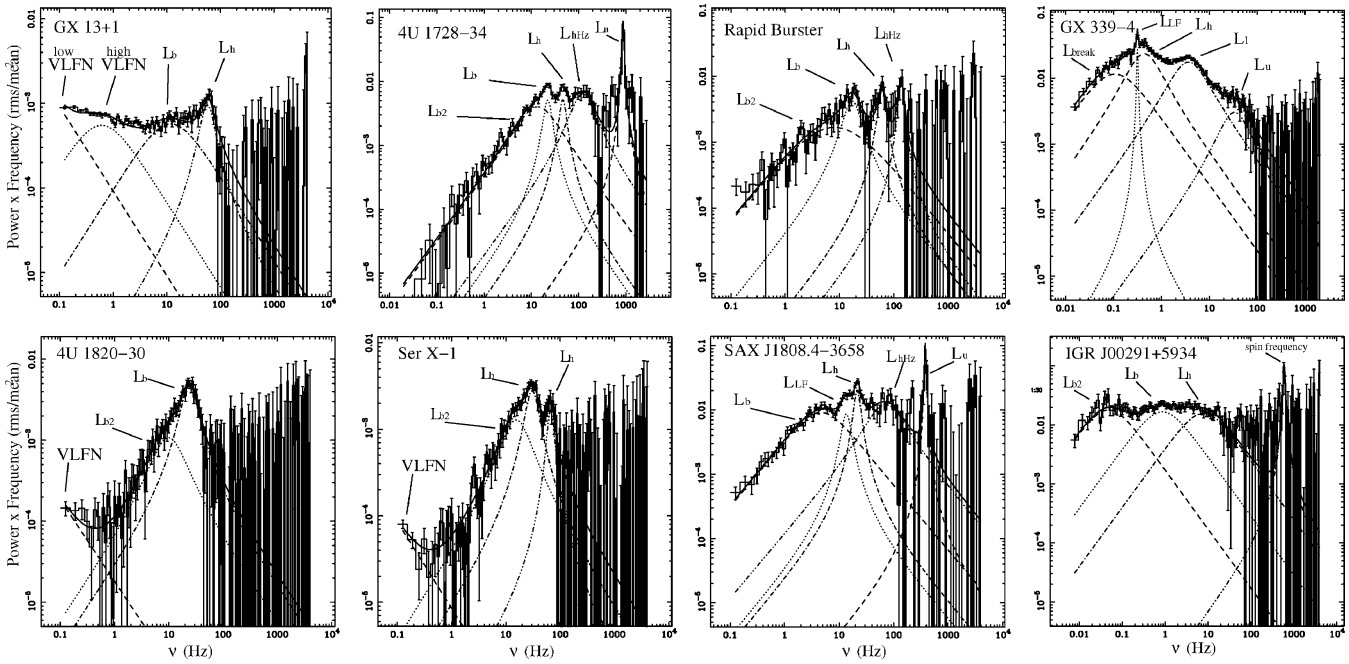

Figure 1. Power density spectra with the fitting multi-Lorentzian model of the NS X-ray binaries analysed: GX 13+1, 4U 1728–34, MXB 1730–335 (the Rapid Burster), 4U 1820–30 and Ser X-1, SAX J1808.4–3658 and IGR J00291+5934, and a typical power spectra of the BH GX 339–4 during the hard state.

MXB 1730–335 (Rapid Burster). Moore et al. (2000) reported the discovery of the radio (transient) counterpart of the Rapid Burster, detected (with the VLA) during two X-ray outbursts in 1996 November and 1997 June. As a result of the large field of view of the PCA, during on-axis pointings of the Rapid Burster the estimated flux is contaminated by the presence of the positionally nearby bright 4U 1728–34. We have therefore analysed slew data of the observation of 1996 November 6, when 4U 1728–34 was no longer in the field of view of the PCA. (The slew observations contemporaneous to the other radio detections do not have enough statistics to identify the components in the power spectra.) We have fitted the power spectrum with four Lorentzians: a broad $L_{\rm b2}$ at ∼8 Hz, and three narrower features at higher frequencies: $L_{\rm b}$ at ∼17 Hz, L_h at ∼60 Hz and $L_{h\ {\rm Hz}}$ at ∼135 Hz (see Fig. 1). The identification of the features has been made by us, using van Straaten et al. (2002, 2003, 2005) and Altamirano et al. (submitted), based on the similarities of the power spectra to that of other atoll sources.

SAX J1808.4–3658. Gaensler et al. (1999) reported the discovery of a radio transient emission (with the Australian Telescope Compact Array: ATCA) from the millisecond accreting X-ray pulsar SAX J1808.4–3658 during the decay of an X-ray outburst on 1998 April 27. Only an upper limit on the radio emission (lower than the detection on April 27) have been found at 8.5 GHz on April 26, suggesting a re-flaring. The power spectrum of the quasi-simultaneous PCA/*RXTE* observation of April 27 allowed one to identify $L_{\rm b}$ at ∼0.8 Hz, but due to the bad statistics above 4 Hz, only a broad not reliably identifiable feature can be fitted around 17 Hz (see also van Straaten et al. 2005). The PCA/*RXTE* observation on April 26 allows one to identify both $L_{\rm b}$ and L_h in the power spectrum. Rupen et al. (2002) reported two radio detections at 8.5 GHz with the VLA, during the peak of the X-ray outburst on 2002 October 16 and 18. In the power spectra of the simultaneous PCA/*RXTE* observations on October 16 and 18 we identified five and six Lorentzian components, respectively: $L_{\rm b2}$ (only on October 18), $L_{\rm b}$, $L_{\rm LF}$, L_h, $L_{h\ {\rm Hz}}$ and $L_{\rm u}$. The identification of the features has been made using van Straaten et al. (2005) and Linares et al. (2005, submitted).

IGR J00291+5934. This millisecond accreting X-ray pulsar (Eckert et al. 2004; see Markwardt, Swank & Strohmayer 2004; Galloway et al. 2005) has been detected in radio band with the Ryle Telescope, at 15 GHz with a flux density of 1.1 mJy almost at the peak of the X-ray outburst (Pooley 2004). The radio emission faded rapidly over the following days (Fender et al. 2004b), suggesting an emission from a discrete relativistic outflow, probably launched at the peak of the X-ray outburst. We have analysed the power spectrum of the PCA/*RXTE* observation of IGR J00291+5934 on 2004 December 7, the first public observation available with quasi-simultaneous radio observations. We could fit the power spectrum with three Lorentzians: $L_{\rm b2}$ at ∼0.05 Hz, $L_{\rm b}$ at ∼0.7 and L_h at ∼5 Hz (see Fig. 1). The identification of the features has been made using van Straaten et al. (2005) and Linares et al. (in preparation).

GX 13+1. The 'peculiar' and persistently bright atoll source GX 13+1 has been observed simultaneously in X-rays (with the PCA/*RXTE*) and radio at 5 GHz (with the VLA) by Homan et al. (2004). They reported a relation between the position on the X-ray colour–colour diagram (CD) and the radio emission behaviour (i.e. flaring emission in the harder state). The classification of GX 13+1 as atoll- or Z-type NS is controversial. GX 13+1 shows many X-ray properties common to both classes, although more similar to atoll sources (Schnerr et al. 2003), but radio properties reminiscent of Z sources (Homan et al. 2004). We have converted the radio flux densities from 5 to 8.5 GHz, assuming a flat spectrum during the steady emission in the soft state, and $\alpha = -0.6$ ($S_\nu \propto \nu^\alpha$, where S_ν is the flux density at a frequency ν) during the flare in the harder state (consistent with observations of radio flares in NSs: e.g. Cooke

& Ponman 1991; Hjellming et al. 1990a,b; Penninx et al. 1993; Fomalont, Geldzahler & Bradshaw 2001). For the identifications of the timing components in the power spectra (Fig. 1), we followed the detailed timing analysis in Schnerr et al. (2003).

GX 339–4. GX 339–4 is one of the two BHs to reveal a correlation between radio and X-ray flux in the hard state over a few orders of magnitude (Corbel et al. 2001; the other is V404 Cyg: Gallo et al. 2003), and the only one to have PCA/*RXTE* observations, simultaneous with ATCA radio observations, which can trace smoothly the X-ray timing behaviour of the source in the hard state over an order of magnitude in radio luminosity. In order to compare the relations between radio emission and X-ray timing among NSs and BHs, we have analysed the simultaneous observations of the BH GX 339–4 reported in Corbel et al. (2000; see Table 1), during the hard state, and which have an optically thick radio spectrum (i.e. a steady compact jet). The identification of the features has been made using Psaltis et al. (1999), Belloni et al. (2002) and Klein-Wolt et al. (in preparation).

Note that previous radio/X-ray timing analysis of other BH XRBs shows in the 'peculiar' BH GRS 1925+105 a relation between the radio states and the QPO centroid frequency, i.e. the frequency is lower during the so-called radio plateau state where the source has a higher optically thick radio flux (Muno et al. 2001), and no evidence for correlations in Cyg X-1, which is almost persistently in the hard state, but steadily at high X-ray luminosities close to the soft state transition (Pottschmidt et al. 2003).

3 RESULTS

We find significant correlations between the radio luminosity $L_{\rm R}$ (at 8.5 GHz and calculated using the distances listed in Table 2) and the X-ray timing features L_h and $L_{\rm b}$ in NS XRBs (Figs 2a–c) and L_ℓ in BH GX 339–4 (Figs 2a′–c′). L_h and $L_{\rm b}$ in the NSs and L_ℓ and $L_{\rm break}$ in the BH have been chosen because they are the components that are almost always present in the power spectra thus allowing a comparison among observations and sources.

Spearman rank tests give positive correlations for $L_{\rm R}$–ν_h (99.2 per cent) and $L_{\rm R}$–$\nu_{\rm b}$ (99.1 per cent) without considering millisecond accreting X-ray pulsars (i.e. with 4U 1728–34, 4U 1820–34, Ser X-1, MXB 1730–335, GX 13+1). Adding also the millisecond accreting X-ray pulsars (IGR J00291+5934 and SAX J1808.4–3658, not shown in Fig. 2 and discussed in more detail in Section 4.2) we still found a significant correlation for $L_{\rm R}$–$\nu_{\rm b}$ (99.3 per cent), but only marginal for $L_{\rm R}$–ν_h (97.4 per cent).

As expected from the negative correlations found between the characteristic frequency and the rms of the Lorentzian components in the power spectra of NS XRBs (e.g. van Straaten et al. 2002, 2003, 2005), we also found a negative correlation between $L_{\rm R}$ and the rms of L_h (99.1 per cent with atoll sources and 99.7 per cent with also millisecond X-ray pulsars) and the rms of $L_{\rm b}$ (98.8 per cent with atoll sources and 99.7 per cent also with millisecond X-ray pulsars).

We fitted all of these correlations with power laws. The fits with a power-law model give χ^2/d.o.f. not better than ∼4 (considering errors on both variables); however, due to a lack of physical models to describe such correlations, the derived fitting parameters, such as the power-law spectral index, are useful for quantifying the relations of these observational quantities. To quantify the likelihood of the power-law model to describe the correlations, we also quote the value of the linear coefficient r calculated for each correlation in a logarithmic scale. In order to be more conservative, we chose to perform the fit considering the atoll sources without the 'peculiar' atoll source GX 13+1. In this way we can trace the behaviour of the other sources (GX 13+1, but also of the millisecond X-ray pulsars) with respect to them (Spearman rank tests without GX 13+1 and the millisecond accreting X-ray pulsars gives: for $L_{\rm R}$–ν_h a significance of 98.7 per cent, for $L_{\rm R}$–$\nu_{\rm b}$ a significance of 98.9 per cent and for $L_{\rm R}$–rms of L_h a significance of 97.7 per cent). In the following we quote the values of the fitting parameters with 1σ errors derived using only errors on $L_{\rm R}$ (similar values are derived using errors on both variables).

Fits with a power law $L_{\rm R} = A \times \nu_{h/b}^{\Gamma}$ of the radio luminosity as a function of the timing frequencies give, for ν_h a slope of $\Gamma = 1.30 \pm 0.10$ and a normalization $A = 10.8 \pm 3.8$, and for $\nu_{\rm b}$ a $\Gamma = 0.63 \pm 0.04$ and $A = 197.1 \pm 17.0$. Note that the $L_{\rm R}$–$\nu_{\rm b}$ correlation looks more 'bimodal' than $L_{\rm R}$–ν_h (Fig. 2c; $r = 0.85$ and 0.93, respectively, for $L_{\rm R}$–$\nu_{\rm b}$ and $L_{\rm R}$–ν_h).

A fit with a power law of $L_{\rm R}$ with the rms of the timing components give, for the rms of L_h: $\Gamma = -2.32 \pm 0.14$ and $A = 7.303(\pm 2.255) \times 10^4$ with a correlation coefficient $r = -0.87$; and for the rms of $L_{\rm b}$: $\Gamma = -1.66 \pm 0.20$ and $A = 7.65 \pm 3.81$ with a correlation coefficient $r = -0.66$.

Correlations similar to those found for ν_h and for the break frequency in NSs also hold for BH GX 339–4 in the hard state. In Fig. 2(a)′ we show the radio luminosity at 8.5 GHz as a function of the characteristic frequency ν_ℓ in BH GX 339–4 (see Section 4.3 for a discussion). The fit with a power law gives $A = (4.88 \pm 0.11) \times 10^3$, and a slope of $\Gamma = 1.37 \pm 0.02$ (the slope is consistent with being the same as with ν_h in atoll NSs). The rms of L_ℓ, as in NSs, decreases with radio luminosity and a power-law fit gives $A = 3.54(\pm 0.45) \times 10^7$ and a slope of $\Gamma = -2.38 \pm 0.03$ (with a correlation coefficient $r = -0.90$; Fig. 2b′). This slope is also consistent with the Γ found for the rms of L_h in atoll NSs. A marginally significant correlation (95 per cent) has been found between the radio luminosity and the break frequency $\nu_{\rm break}$ (Fig. 2c′). A power-law fit (without the upper limit point) gives $\Gamma = 0.87 \pm 0.02$ and $A = 2.59(\pm 0.99) \times 10^5$, with a linear correlation coefficient of $r = 0.88$.

As a caveat we note that, in NSs, in the case of a transient outburst, X-ray and radio emission may have been decoupled. X-ray timing features, being related to the disc properties, should be a more reliable tracer of the compact steady continuous replenished jet, rather than of the evolution of a transient optically thin jet, at least after the jet has been launched and thus decoupled from the disc. In this context, this caveat specifically applies to the millisecond accreting X-ray pulsar SAX J1808.4–3658 detected in the radio band only during X-ray outbursts that do not, in fact, follow the $L_{\rm R}$–ν_h correlation found for the other sources (Fig. 3; see Section 4.2). The fact that the data of the (likely) transient jet in the Rapid Burster (and actually also the millisecond accreting X-ray pulsar IGR J00291+5934 which is in the last part of the X-ray outburst decay) instead do lie on the radio–X-ray timing correlations may suggest a continuity in power between the compact and the transient jet at launch (see the discussion in Fender, Belloni & Gallo 2004a for BHs).

4 DISCUSSION

We have analysed all of the available PCA/*RXTE* observations coordinated with the radio band, of atoll NSs and millisecond accreting X-ray pulsars with a detected radio counterpart.

We find significant correlations between the radio luminosity at 8.5 GHz and X-ray timing features. We compared these relations in NSs with those of the BH GX 339–4 in the hard state, for which we could smoothly follow the radio behaviour and the high-resolution

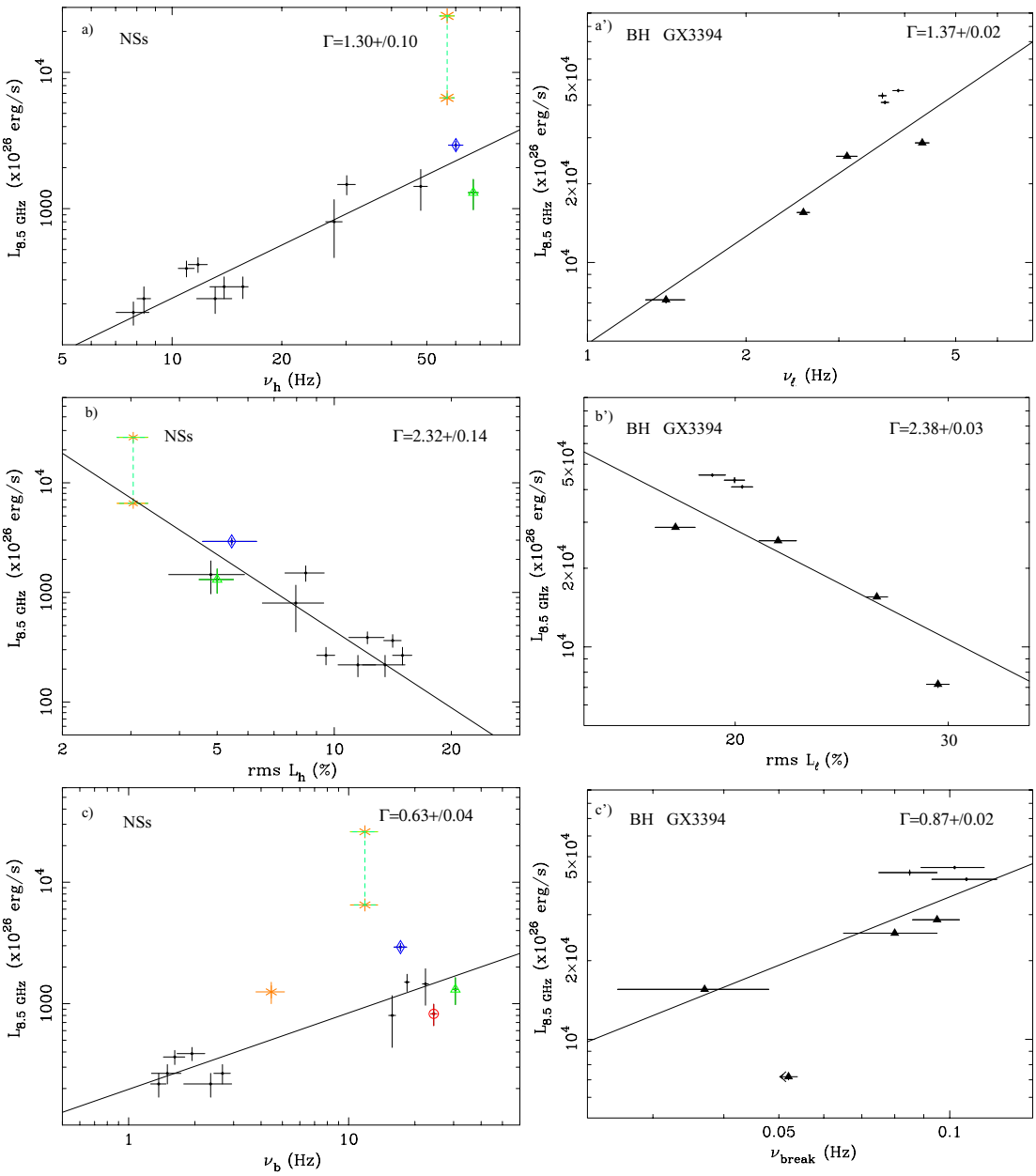

Figure 2. Top panels, radio luminosity at 8.5 GHz as a function of the characteristic frequency ν_h for NSs (a) and of ν_ℓ for the BH GX 339–4 (a′); middle panels, radio luminosity at 8.5 GHz as a function of the rms of L_h for NSs (b) and the rms of L_ℓ for the BH GX 339–4 (b′); lower panels, radio luminosity at 8.5 GHz as a function of $\nu_{\rm b}$ for the NSs (c) and $\nu_{\rm break}$ for the BH GX 339–4 (c′). NSs are 4U 1728–30 (dots), Ser X-1 (open triangle), the Rapid Burster (open diamond), 4U 1820–30 (open circle) and the 'peculiar' atoll GX 13+1 (asterisks; the dashed vertical line indicates the range in radio luminosity observed during the flare, while the timing frequency has been estimated by averaging the whole X-ray observation; see Homan et al. 2004). In the BH GX 339–4 we marked with dots the observations in the hard state before the 1998 X-ray outburst, and with triangles the observations in the hard state after the outburst. The upper limit on the $\nu_{\rm break}$ frequency in panel c′ is the characteristic frequency ν_h (see Table 1). The slope Γ of the fitting power laws (solid lines; GX 13+1 has been excluded from the fit, see Section 3) are indicated on the top right-hand corner of each panel (see Section 3).

X-ray timing variations over an order of magnitude in the radio luminosity. We found that similar relations hold in the two different classes of sources. In particular, we observe in atoll NSs correlations between the radio luminosity and L_h and between radio luminosity and the break frequency component $L_{\rm b}$, in BHs correlations between radio luminosity and L_ℓ and (marginally) between radio luminosity and the break frequency $L_{\rm break}$. In the following we will discuss some implications of these results and suggest possible scenarios, which require testing using a larger sample.

4.1 Atoll-type NSs

The phenomenon of the parallel tracks in the X-ray luminosity versus kHz QPO frequency plot for NSs (e.g. Méndez et al. 1999; see van der Klis 2005 for a review) may be explained using a single time-dependent physical quantity, usually inferred as the mass accretion rate in the disc $\dot{M}_{\rm d}$, if we consider the kHz QPO frequency to be governed by the balance between this quantity and luminosity $L_{\rm X}$, while the luminosity responds to both this quantity and its

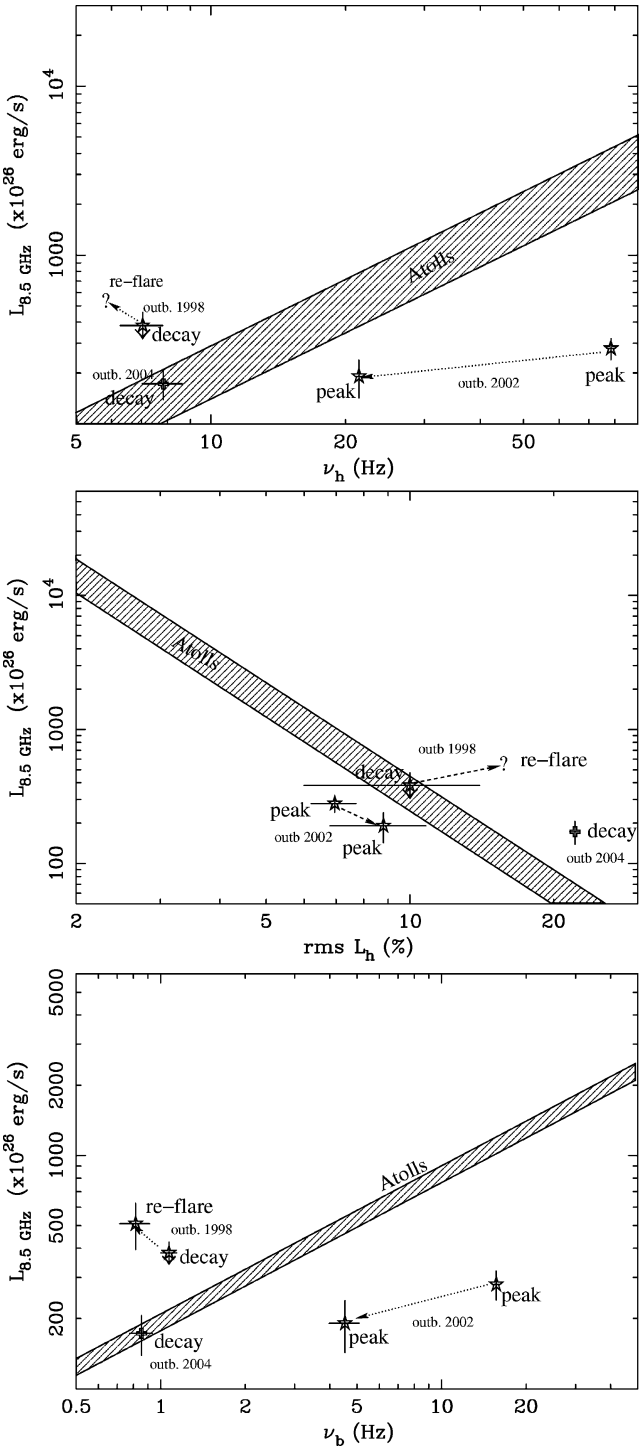

Figure 3. Radio luminosity at 8.5 GHz as a function of ν_h (upper panel), the rms of L_h (middle panel) and ν_b (lower panel) for the millisecond accreting X-ray pulsars IGR J00291+5934 (open cross) and SAX J1808.4–3658 (stars). The grey region represent the power-law fit to the atoll sources considering 1σ errors on the normalization A only [e.g. $S_{8.5} = A \times (\nu)^{\Gamma}$; see Section 3]. The question mark indicates an uncertainty on ν_h, because as no L_h could be identified on 1998 April 27, we used the value of the X-ray observation closest to that day and for which ν_b was consistent with that on 1998 April 27 (i.e. group number 21 in van Straaten et al. 2005; see also Section 2.2). The arrows indicate the chronological sequence of the observations during each X-ray outburst.

time-averaged variations (van der Klis 2001). The QPOs seem to be a good tracer of the disc geometry as determined by the balance between $\dot{M}_d$ and L_X, in the regions very close to the compact object where jets are also thought to originate (see also below). van der Klis (2001) also suggested that one possible mechanism for balancing the energy budget is by removing material from the binary in the form of a mildly relativistic jet, so that the accretion rate on to the compact object is no longer the same as the mass transfer rate through the disc.

All the variability components in the power spectra follow a universal scheme, when plotted against the upper-kHz QPO. Therefore, the disc geometry may also be inferred by low-frequency timing features. In particular, in atoll sources, a tight correlation exists between the centroid frequency of the upper-kHz QPO and that of (the radio power tracer) L_h: the best-fitting power law is $\nu_{h,0} \propto \nu_{u,0}^2$ (van Straaten et al. 2003) or $\nu_h \propto \nu_u^{2.4}$ using ν_{max} (van Straaten et al. 2005). If we assume that ν_u is related to an orbit in the disc at an inner radius R_{in}, the fact that the radio jet power increases with ν_h may be explained by a scenario in which the jet particles and magnetic field lines may be 'squeezed' as the disc moves inwards. (The jet power possibly increases until the magnetic field lines of the jet interact with the magnetic field of the NS surface; see also below in Section 4.2.)

4.2 Millisecond accreting X-ray pulsars

The observations of the millisecond accreting X-ray pulsar IGR J00291+5934, taken in the last part of the decay of the X-ray outburst on 2004, also lies on the radio luminosity/X-ray timing frequency correlations of atoll sources (adding this source the L_R–ν_b and L_R–ν_h rank correlations are significant to the 99.6 and 99.7 per cent level, respectively). In contrast, the observations of SAX J1808.4–3658 seem to diverge from the radio/X-ray coupling found in atoll sources and IGR J00291+5934, especially from the L_R–ν_h relation (see Section 3; note that the millisecond X-ray pulsars are still consistent with the rank correlations between radio luminosity and the rms of the X-ray timing features of atolls sources; see also Fig. 3, middle panel). The radio upper limit of SAX J1808.4–3658 has been derived on 1998 April 26 from an observation during the last part of the decay of an X-ray outburst, as for IGR J00291+5934, and this value is also consistent with the correlations of the atolls. The observations that do not lie on the radio luminosity/X-ray timing frequency correlation are those of SAX J1808.4–3658 taken during the peak of the outburst in 2002 and the one that apparently reflared on 1998 April 27. Although the lack of observations does not yet allow a complete understanding of the behaviour of the simultaneous radio/X-ray emission of millisecond X-ray pulsars throughout the evolution of an X-ray outburst, based on the present data we can start to make some remarks and speculations.

Focusing on the radio luminosity/X-ray timing frequency relations (Fig. 3, upper and lower panels) we see that when the frequency is high ($\nu_h > 20$; $\nu_b > 4$) the radio luminosity is below that expected from atoll sources, while it is above during the re-flaring when the source shows lower timing frequencies. Furthermore, we see that in the 2002 outburst, over 2 d the timing frequencies change of a factor of 4, while only a slight decrease is observed in radio luminosity, i.e. an increase in radio loudness. This may be an indication of an actual decoupling of the disc and the jet during the outburst, thus a signature that a discrete jet has been launched. The fact that when the timing frequencies are higher the source is less radio-loud than at lower timing frequencies, may be due to the relative importance

of the magnetic field of the NS when the disc is getting closer to the NS during the outburst. For the two observations in 2002 we have a direct measurement of the upper-kHz QPOs: $L_{\rm u} \sim 700$ Hz on October 16 and $L_{\rm u} \sim 400$ Hz on October 18 (see also van Straaten et al. 2005). If we relate this frequency to the Keplerian orbit in the disc at a radius $R_{\rm in}$, for a 1.4-$M_\odot$ NS we derive $R_{\rm in} \sim 70$ km in the October 16 observation and $R_{\rm in} \sim 100$ km in the October 18 observation. For the observation of 1998 April 27, using the relation $\nu_h \propto \nu_{\rm u}^{2.4}$ we derive $R_{\rm in} \sim 140$ km. In millisecond accreting X-ray pulsars the magnetic field of the NS might be higher than in atoll NSs (e.g. Chakrabarty 2005), and for SAX J1808.4–3658 it has been estimated to be $\sim 10^8$–10^9 G (Psaltis et al. 1999). The (as yet poor) observations may suggest that below, say, $\sim 10^2$ km from the NS, the magnetic field, interacting more strongly with the regions of the disc where the jet is formed – closer to the compact object as the jet becomes more powerful as suggested by the correlation with the X-ray timing frequencies – suppresses in some way the power of the jet (possibly by interfering with a magnetic expulsion mechanism; see also Section 4.1). We can have a rough estimate of the radius at which this happens if we assume that this interaction is strong when this region is close to the Alfvén radius $R_{\rm A}$. Assuming for SAX J1808.4–3658 a magnetic field at the surface of $\sim 5 \times 10^8$ G (Psaltis & Chakrabarty 1999), a luminosity during the decay of the 1998 outburst on April 27 of $\sim 3 \times 10^{35}$ erg s^{-1} [from Gilvanov et al. (1998), using a distance of 2.5 kpc (in't Zand et al. 2001)] and a radius of the NS of $\sim$10 km (Burderi & King 1998), we obtain $R_{\rm A} \sim 110$ km, and slightly smaller radii for the other observations (see, e.g., Frank, King & Raine 2002 and references therein). This radius is consistent with the inner radius we have estimated with frequencies of kHz QPOs, therefore suggesting that the magnetic field of the NS, through its interaction with the innermost regions of the accretion disc, might also play a role in (e.g. inhibiting) the production of the jet.

4.3 NSs and BHs

Casella, Belloni & Stella (2005) found a clear association between a low-frequency QPO, the so-called type-C QPO in BHs (e.g. Wijnands et al. 1999; Remillard et al. 2002; Casella et al. 2004) and the horizontal-branch oscillation (HBO) in Z-type NSs, suggesting a similar physical origin for these two timing features. van Straaten et al. (2003) already compared the low-frequency features of atolls with those of Z sources, and, based upon the correlation with the frequency of the kHz QPOs, identified the HBO in Z sources with L_h in atoll sources. [Note that, a correlation between radio power and the position in the CD has been found in Z sources, and it is precisely in the HB that Z sources are more radio-loud (Penninx et al. 1988; Hjellming et al. 1990a,b).] In BHs, Psaltis et al. (1999; see also fig. 12 in Belloni et al. 2002) found a tight almost *linear* correlation between the frequencies of the narrow low-frequency QPO $L_{\rm LF}$ (i.e. also the type-C QPO) and a broader component that they called L_ℓ (reminiscent of the lower-kHz component in NSs). Using these known relations we can (linearly) associate L_h of NSs with L_ℓ of BHs (where the choice for these two features has been dictated by availability in the power spectra of our sample; see Section 3). The fact that we find for these two features the same scaling with radio luminosity supports the idea that the same physics lies behind their origin.

As all the compact jet models predict that the total jet power $L_{\rm J}$ and the power radiated in radio $L_{\rm R}$ are related as $L_{\rm R} \propto L_{\rm J}^{1.4}$ (e.g. Blandford & Königl 1979; Falcke & Biermann 1996; Falcke, Markoff, Falcke & Fender 2001), the finding that the radio luminosity scales with ν_h and ν_l, in NSs and BHs, respectively, with a slope of $\Gamma \sim 1.3$–1.4, would imply an almost linear correlation of $L_{\rm J}$ with these timing features.

It is interesting to note that if we consider the frequencies of the timing components correlated with the radio luminosity (i.e. ν_h for NSs and ν_ℓ for BH GX 339–4) as originating from Keplerian motion of matter in the disc, from the dynamical time-scales observed we derive a distance to the compact object of $\sim$100–300 and 100–500 $R_{\rm Schw}$ (where $R_{\rm Schw} = 2GM/c^2$ is the Schwarzschild radius), respectively, in NSs and in GX 339–4. These radii are consistent with those derived from high-resolution radio imaging of the active galaxy M87 (Junor, Biretta & Livio 1999) and consistent with the idea that jets are formed very close to the compact object.

The relations between the radio luminosity and the break frequency are even more intriguing, because such features have also been observed in active galactic nuclei (AGN) (e.g. McHardy et al. 2004). Therefore, these correlations, if further confirmed especially with a larger sample of BHs, open up the possibility of the existence of a new 'fundamental plane' for XRBs and AGN (Merloni, Heinz & Di Matteo 2003), where the dimensions are the mass of the compact object, the radio luminosity and the characteristic frequency of a timing feature (e.g. break), the last being, contrary to the X-ray luminosity (see Merloni et al. 2003; Falcke, Körding & Markoff 2004), independent from the distance to the source. X-ray timing features can be the key features to finally finding the common physical link between the accretion disc and the jet radio emission in NSs and BHs of all masses.

ACKNOWLEDGMENTS

We thank the anonymous referee for her/his useful suggestions. We acknowledge useful conversations with Phil Uttley. SM would like to thank Rudy Wijnands, Tomaso Belloni, Marc Klein-Wolt, Diego Altamirano and Manuel Linares for very helpful discussions.

REFERENCES

Altamirano D., van der Klis M., Méndez M., Migliari S., Jonker P. G., Tiengo A., Zhang W., 2005, ApJ, in press (astro-ph/0507097)
Blandford R. D., Konigl A., 1979, ApJ, 232, 34
Belloni T., Psaltis D., van der Klis M., 2002, ApJ, 572, 392
Burderi L., King A. R., 1998, MNRAS, ApJ, 505, L135
Casella P., Belloni T., Homan J., Stella L., 2004, A&A, 426, 587
Casella P., Belloni T., Stella L., 2005, A&A, 629, 403
Chakrabarty D., 2005, in Rasio F. A., Stairs I. H., eds, Binary Radio Pulsars, ASP Conf. Ser. Astron. Soc. Pac., San Francisco (astro-ph/0408004)
Cooke B. A., Ponman T. J., 1991, A&A, 244, 358
Corbel S., Fender R. P., Tzioumis A. K., Nowak M., McIntyre V., Durouchoux P., Sood R., 2000, A&A, 359, 251
Corbel S., Nowak M. A., Fender R. P., Tzioumis A. K., Markoff S., 2003, A&A, 400, 1007
Eckert D., Walter R., Kretschmar P., Mas-Hesse M., Palumbo G. G. C., Roques J.-P., Ubertini P., Winkler C., 2004, The Astronomer's Telegram, 352
Falcke H., Biermann P. L., 1996, A&A, 308, 321
Falcke H., Körding E., Markoff S., 2004, A&A, 414, 895
Fender R. P., 2005, in Lewin W. H. G., van der Klis M., eds, Compact Stellar X-Ray Sources. Cambridge Univ. Press, Cambridge (astro-ph/0303339)
Fender R. P., Belloni T., Gallo E., 2004a, MNRAS, 355, 1105
Fender R. P., de Bruyn G., Pooley G. G., Stappers B., 2004b, The Astronomer's Telegram, 361
Fomalont E. B., Geldzahler B. J., Bradshaw C. F., 2001, ApJ, 558, 283
Ford E. C., van der Klis M., Méndez M., Wijnands R., Homan J., Jonker P. J., van Paradijs J., 2000, ApJ, 537, 368

Frank J., King A., Raine D., 2002, Accretion Power in Astrophysics. Cambridge Univ. Press, Cambridge
Gaensler B. M., Stappers B. W., Getts T. J., 1999, ApJ, 522, L117
Gallo E., Fender R. P., Pooley G. G., 2003, MNRAS, 344, 60
Galloway D. K., Psaltis D., Chakrabarty D., Muno M. P., 2003, ApJ, 590, 999
Galloway D. K., Markwardt C. B., Morgan E. H., Chakrabarty D., Strohmayer T. E., 2005, ApJ, 629, L45
Gilfanov M., Revnivtsev M., Sunyaev R., Churazov E., 1998, A&A, 338, L83
Hasinger G., van der Klis M., 1989, A&A, 225, 79
Heasley J. N., Janes K. A., Zinn R., Demarque P., Da Costa G. S., Christian C. A., 2000, AJ, 120, 879
Heinz S., Sunyaev R. A., 2003, MNRAS, 343, L59
Hjellming R. M., Han X. H., Córdova F. A., Hasinger G., 1990a, A&A, 235, 147
Hjellming R. M. et al., 1990b, ApJ, 365, 681
Homan J., Belloni T., 2005, in Maccarone T. J., Fender R. P., Ho L., eds, Proc. of From X-ray Binaries to Quasars: Black Hole Accretion on all Mass Scales. Kluwer, Dordrecht, in press (astro-ph/0412597)
Homan J., Wijnands R., van der Klis M., Belloni T., van Paradijs J., Klein-Wolt M., Fender R. P., Méndez M., 2001, ApJ, 132, 377
Homan J., Wijnands R., Rupen M. P., Fender R. P., Hjellming R. M., Di Salvo T., van der Klis M., 2004, A&A, 418, 255
in't Zand J. J. M. et al., 2001, A&A, 372, 916
Jonker P. G., Nelemans G., 2004, MNRAS, 354, 355
Junor W., Biretta J. A., Livio M., 1999, Nat, 401, 891
Klein-Wolt M., 2004, PhD thesis, Univ. of Amsterdam
Kuulkers E., den Hartog P. R., in't Zand J. J. M., Verbunt F. W. M., Harris W. E., Cocchi M., 2003, A&A, 399, 663
Leahy D. A., Darbro W., Elsner R. F., Weisskopf M. C., Kahn S., Sutherland P. G., Grindlay J. E., 1983, ApJ, 266, 160
Linares M., van der Klis M., Altamirano D., Markwardt C. B., 2005, ApJ, in press
McClintock J. E., Remillard R. A., 2005, in Lewin W. H. G., van der Klis M., eds, Compact Stellar X-Ray Sources. Cambridge Univ. Press, Cambridge
McHardy I. M., Papadakis I. E., Uttley P., Page M. J., Mason K. O., 2004, MNRAS, 348, 783
Markoff S., Falcke H., Fender R. P., 2001, MNRAS, A&A, 372, L25
Markwardt C. B., Swank J. H., Strohmayer T. E., ATEL, 353
Méndez M., van der Klis M., Ford E. C., Wijnands R., van Paradijs J., 1999, ApJ, 511, L49
Merloni A., Heinz S., Di Matteo T., 2003, MNRAS, 345, 1057
Migliari S., Fender R. P., Rupen M., Jonker P. G., Klein-Wolt M., Hjellming R. M., van der Klis M., 2003, MNRAS, 342, L67
Migliari S., Fender R. P., Rupen M., Wachter S., Jonker P. G., Homan J., van der Klis M., 2004, MNRAS, 351, 186
Miller J. M., Homan J., 2005, ApJ, 618, L107
Moore C. B., Rutledge R. E., Fox D. W., Guerriero R. A., Lewin W. H. G., Fender R. P., van Paradijs J., 2000, ApJ, 532, 1181
Muno M. P., Remillard R. A., Morgan E. H., Wallman E. B., Dhawan V., Hjellming R. M., Pooley G. G., 2001, ApJ, 556, 515
Narayan R., Yi I., 1994, ApJ, 428, L13
Narayan R., Yi I., 1995, ApJ, 444, 231
Narayan R., Garcia M. R., McClintock J. E., 1997, ApJ, 478, L79
Penninx W. et al., 1988, Nat, 336, 146
Penninx W., Zwarthoed G. A. A., van Paradijs J., van der Klis M., Lewin W. H. G., Dotani T., 1993, A&A, 267, 92
Pooley G. G., 2004, The Astronomer's Telegram, 355
Pottschmidt K. et al., 2003, A&A, 407, 1039
Psaltis D., Chakrabarty D., 1999, ApJ, 521, 332
Psaltis D., Belloni T., van der Klis M., 1999, ApJ, 520, 262
Remillard R. A., 2005, in Chen P., ed., SLAC Electronic Conf. Proc. Archive. In press (astro-ph/0504129)
Remillard R. A., Sobczak G. J., Muno M. P., McClintock J. E., 2002, ApJ, 564, 962
Rupen M. P., Dhawan V., Mioduszewski A. J., Stappers B. W., Gaensler B. M., 2002, IAU Circ., 7997, 2
Rupen M. P., Mioduszewski A. J., Dhawan V., 2004, The Astronomer's Telegram, 286
Rutledge R., Moore C., Fox D., Lewin W. H. G., van Paradijs J., 1998, IAU Circ., 6813, 2
Schnerr R. S., Reerink T., van der Klis M., Homan J., Meńdez M., Fender R. P., Kuulkers E., 2003, A&A, 406, 221
Tan J., Lewin W. H. G., Hjellming R. M., Penninx W., van Paradijs J., van der Klis M., Mitsuda K., 1992, ApJ, 385, 314
van der Klis M., 1989, ARA&A, 27, 517
van der Klis M., 1995, in Alpar M. A., Kiziloglu U., van Paradijs J., eds, Proc. NATO Advanced Study Institute on the Lives of Neutron Stars. Kluwer, Dordrecht
van der Klis M., 2001, ApJ, 561, 943
van der Klis M., 2005, in Lewin W. H. G., van der Klis M., eds, Compact Stellar X-Ray Sources. Cambridge Univ. Press, Cambridge, in press (astro-ph/0410551)
van Straaten S., van der Klis M., Di Salvo T., Belloni T., 2002, ApJ, 568, 912
van Straaten S., van der Klis M., Méndez M., 2003, ApJ, 596, 1155
van Straaten S., van der Klis M., Wijnands R., 2005, ApJ, 619, 455
Wijnands R., Homan J., van der Klis M., 1999, ApJ, 526, L33
Zdziarski A. A., Gierlinski M., Mikolajewska J., Wardziński G., Smith D. M., Alan B., Kitamoto S., 2004, MNRAS, 351, 791
Zhang W., Jahoda K., Swank J. H., Morgan E. H., Giles A. B., 1995, ApJ, 449, 930

This paper has been typeset from a TEX/LATEX file prepared by the author.